Manifestation of space weather effects in atmospheric electric parameter variations at a mid-latitudinal* observatory

Sergey Smirnov*

Institute of Cosmophysical Research and Radio Wave Propagation FEB RAS, Russia.

ABSTRACT: The following changes occurred during solar events and magnetic storms in the diurnal variations of air electric conductivity, electric field strength and meteorological values in the near ground atmosphere in Kamchatka. Air electric conductivity decreased that was associated with galactic cosmic ray flux decrease, the Forbush effect. Storm sudden commencement caused induction effects in the electric fields. Intensification of the components with the period of 48 hours in air electric conductivity power spectra and electric field strength was observed. The same effect manifested in the power spectra of galactic cosmic rays and of atmospheric pressure that indicates planetary scale atmospheric waves excitation during solar events.

INTRODUCTION

In fair weather conditions, within the framework of the model for ball condenser formed by the Earth surface and the ionosphere lower boundary, the conductivity current in the global electric circuit (GEC) is determined by remote lightning sources, the so called global lightning generator. Besides, there are other additional generators of global scale, they are: ionospheric generator (in dynamo-region at h ~ 100-120 km), magnetospheric generator and solar cosmic rays (SCR) in the upper atmosphere of polar regions as well as galactic cosmic rays (GCR) in the middle atmosphere (h ~ 15-25 km).

In the near ground atmosphere of mid-latitudes, local current sources contribute as parts of the GEC besides the global sources. They are: convective generator and seismic-nature generator which supplies the radioactive gas Rn into the atmosphere. Cumulus clouds negatively charged in their bottom part are also referred to local generators. It is known that local generators strongly depend on whether parameters (air temperature, pressure, humidity and wind velocity), which in their turn depend on solar activity. Ionospheric dynamo contributes insignificantly to the atmospheric parameters (~5-10%) [Roble, 1985]. We should neglect the magnetospheric generator effect at mid-latitudes in the near ground atmosphere in fair weather conditions. Even in the polar latitudes, the contribution of the magnetospheric generator is ~ 20% in comparison to the lightning generator effect [Roble,1985].

During strong solar flares and geomagnetic storms, their influence as global processes manifests, first of all, in the variations of current global sources in GEC. The results of analysis for these effects at the

*Contact information: Sergey Smirnov, Institute of Cosmophysical Research and Radio Wave Propagation FEB RAS, Russia, Email: sergey@ikir.ru

middle and high latitudes are presented in numerous papers and are subsequently viewed in the articles [Roble, 1985; Rycroft et al., 2012], including the solar event in August 1972.

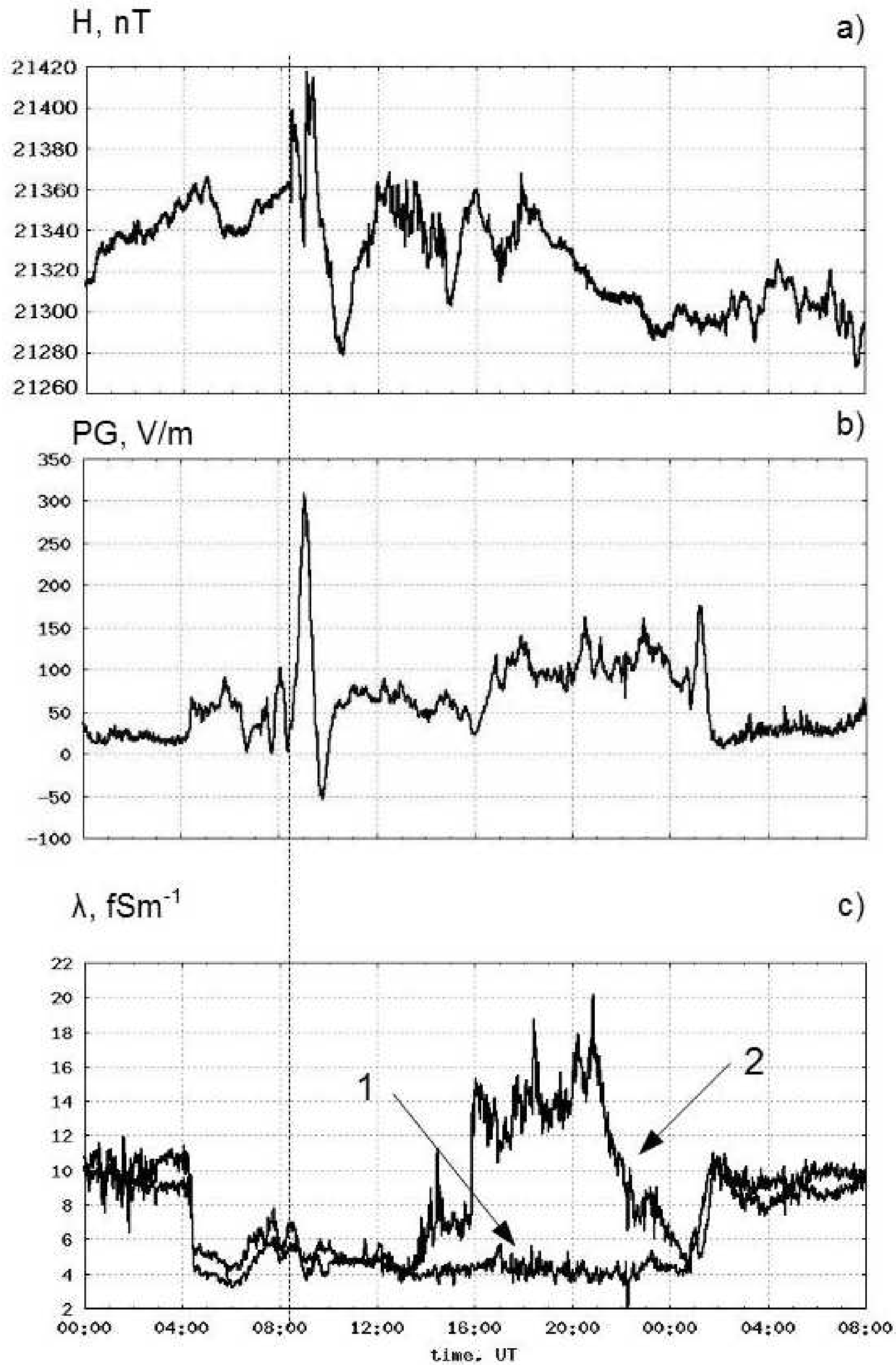

Fig. 1. One-minute averaged data for the geophysical field measurements. Development of the geomagnetic storm (dashed line shows the beginning) on 5 to 6 April 2010 and measurements of the (a) magnetic field H-component, (b) potential gradient, and (c) air electroconductivity caused by negative (1) and positive (2) ions.

METHODS

Observations of geophysical fields were carried out at Paratunka observatory of the Institute of Cosmophysical Research and Radio Wave Propagation FEB RAS, Kamchatka (λ =158.25°E; φ =52.9°N). It is located on a plain, 15 km from the ocean, at an altitude of 50 m above the sea level. Measurements of PG were realized by the 'Pole-2' sensor, which was developed at a Branch of the Voeikov Main Geophysical Observatory [Imyanitov, 1957]. The Pole-2 sensor was installed 200 m from the administration building at a height of 3 m, and the area for it (radius of 12 m) was cleared from trees. After digitization by a 14-bit analog-to-digital converter (ADC), the signal at the output of this fluxmeter was recorded on a personal computer (PC) hard disc with 1-s sampling rate. Simultaneously, air electrical conductivity was measured by an 'Elektroprovodnost-2' unit that was also developed at the Branch of the Main Geophysical Observatory. The unit has two inlets at the height of 3 m so that it can measure electrical conductivity caused by positive and negative air ions separately.

RESULTS

The minimum of the 23-d cycle of solar activity was in December 2008. The period 2006 to 2010 was characterized by a small number of magnetic storms. On 3 April 2010, an X-ray flare of the B7.4 class occurred on the Sun, which led to coronal filament ejection. Its intensity was not big, but it was quite long (more than 7 h). On 5 April 2010 at 8:27 UT, the beginning of a magnetic storm with a sudden commencement was registered. Fig. 1 shows the 1-min averaged data for the geophysical field measurements at the Paratunka site. Fig. 1a shows the graph of the geomagnetic field H-component on 5 to 6 April. The K-index of the storm was 7. A previous storm of the same class occurred on 11 October 2008, i.e., the analyzed event was the strongest storm for the previous year and a half.

Magnetic storm effects on the near-ground electric state may be divided into three stages [Smirnov, 2014]. The background level of PG before the storm was about 25 V/m (Fig. 1b). Field low level is determined by the seasonal variation of high amplitudes from 60 ± 40 to 120 ± 60 V/m. For this month at this observatory, the field low level was characteristic, i.e., there was nothing unusual about it. For example, the paper by Siingh [Siingh et al., 2013] showed PG diurnal variation at different sites during various seasons in the range from 48 to 82 V/m andto from 130 to 185 V/m. The first stage from 4:25 until to 8:27 UT was characterized by an increase of the electric field level up to 50 V/m. Simultaneously, the air electroconductivity experienced a twofold decrease (Fig. 1c). The cause for such an increase in the PG might have been the sharp decrease of the GCR penetration level to Earth's surface. Two factors support this interpretation. First, conduction current density variations during this period were not as significant as during the following time interval and did not change considerably (Fig. 2b). This value was received by an indirect method from the calculation $j = Ez \times (\lambda_+ + \lambda_-)$, where Ez is the electric field strength, and λ_+ and λ_- represent the electroconductivity of the air caused by positive and negative ions, respectively. Second, air electroconductivity sharply decreased during this period (Fig. 1c). The GCRs together with radon are air ionizers. A decrease in the GCR ionization effect leads to a decrease in the electroconductivity (Fig. 1c) and, consequently, to an increase of PG (Fig. 1b). There is no station for cosmic ray measurements in Kamchatka and nearby regions. Fig. 3 shows the data for the proton flux according to GOES-15 data and cosmic ray indices of Moscow. The data were received from the National Geophysical Data Center site: spidr.hgdc.noaa.gov. It is possible that ionization processes in the near-ground layer of mid-latitudes are so complicated and nonlinear that they had such an effect in Kamchatka.

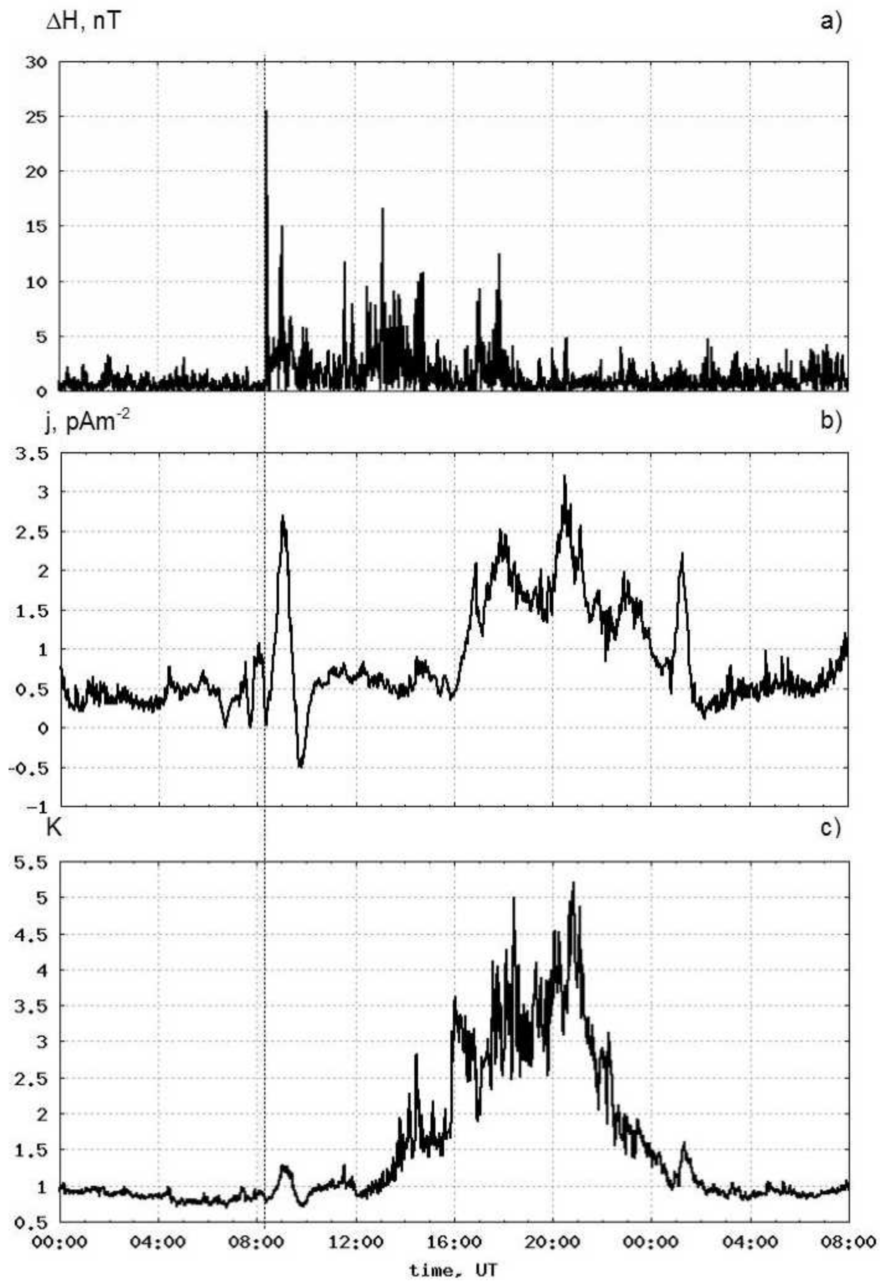

Fig. 2. Development of the geomagnetic storm and graphs of measurements. Development of the geomagnetic storm (dashed line shows the beginning) on 5 to 6 April 2010 and measurements of the (a) magnetic field ΔH, (b) conduction current density, and (c) air unipolarity (λ+/λ-)

During the second stage in the interval from about 8:27 to 12:00 UT, a sharp increase in the electric field and then a decrease occurred. This coincided in time with sharp oscillations of the geomagnetic field H-component, and a similar behavior was observed in the conduction current density. Such disturbances are likely to have an induction nature.

Fig. 2c shows the graph of magnetic field measurements $\Delta H_i = H_{i+1} - H_i$, where H_i is the measurement series of the magnetic field H-component with 1-min averaging. Fig. 2b shows the conduction current density. It is clear from Fig. 2 that the storm with sudden commencement significantly changed the current system in the near-ground layer. But during the following stages, the magnetic disturbance effect on the current system was weak.

At the third stage from about 12:00 UT on 5 April to 1:30 UT on 6 April, an electric field increase occurred, which was associated with an increase of the unipolarity coefficient (Fig. 2c). The unipolarity coefficient $K = \lambda_+/\lambda_-$ takes into account the ion concentration and ion mobility. Observations at the Paratunka observatory show that the rain effect causes a decrease in the unipolarity coefficient, and the snowfall effect causes an increase. The vertical current density during this time exceeded the level of the second stage (Fig. 2b).

It is reasonable to consider the reaction of electric and meteorological processes in the near ground atmosphere on a powerful geomagnetic storm by the method of epoch superposition together with the processes occurring on the Sun and by the Earth surface [Smirnov et al., 2014]. Thus, in Fig. 3 we illustrate the results of observation of different geophysical and meteorological values from 21 to 31 October 2003.

Curves 1 – quasi-static electric field potential gradient measured by Pole-2 unit with the accuracy of 0,3 V/m and 1-minute time discreteness, and Dst-index (nT) determined with 1-hour time discreteness.

Curves 2 and 3 – air electrical conductivity determined separately by positive λ_+ and negative λ_- ions and measured by Electroprovodnost'-2 (in conditional units) device.

Curves 4-8 – pressure (P, gPa); temperature (T, ^{0}C); air humidity (%); precipitation and wind velocity (V, m/s), respectively, measured with 10-minute time discreteness at Paratunka observatory by digital weather stations WS-2000 and WS-2300. The output data are directed to the observatory via a radio channel at the frequency of 433 MHz. Geomagnetic field horizontal component (H) is also plotted on curve 4. It was measured at Paratunka observatory by a fluxgate magnetometer FRG-601G with the accuracy of 0.01 nT and with 1-minute time discreteness (ordinate right axis).

We also applied the data on cloudiness state and on precipitation at the local weather station. Unfortunately, there were no actinometric measurements during that period.

Curve 7 – Kp-index three-hour values.

Curve 9 – Galactic cosmic rays (N is the particle number/min), measured by a neutron monitor with 1-minute discreteness at Stekol'ny observatory of IKIR FEB RAS.

Curve 10 – sequence of solar flares measured on GOES-12 satellite (http://goes.ngdc.noaa.gov/data/avg).

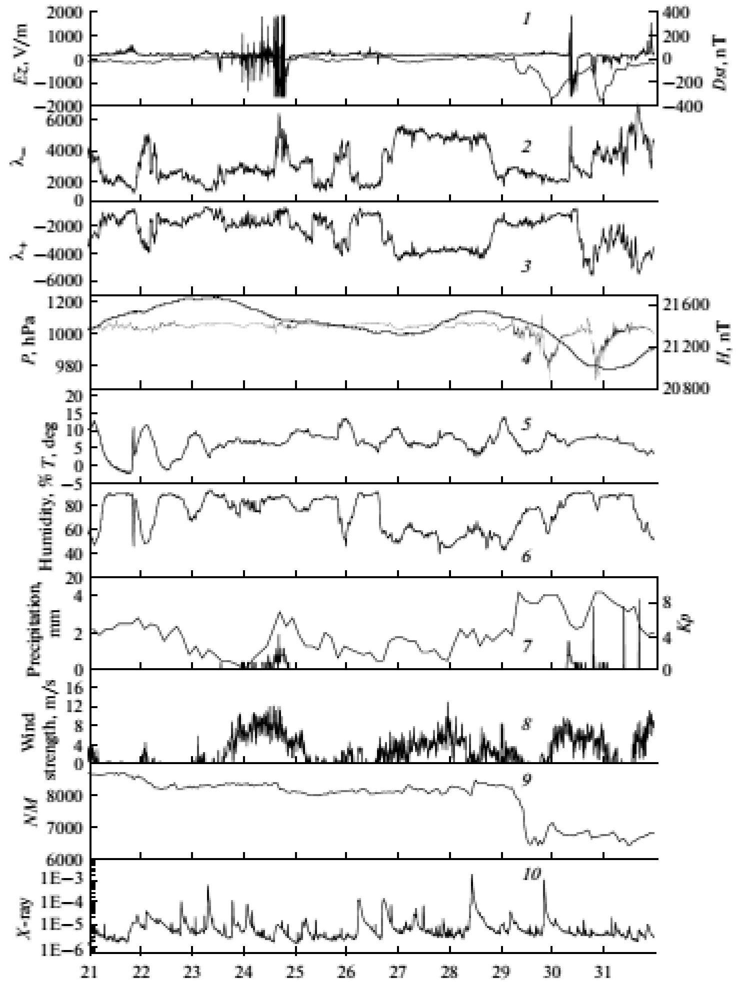

Fig. 3. Diurnal variations in the electric field, electrical conductivity of the atmosphere, meteorological, geophysical and solar variations on October 21–31, 2003.

Fig. 4 and 5 show the power spectra of the values in Fig. 3 selected for the following time intervals: October 21-22, fair weather days; October 22-23, the period of increased solar activity with a series of solar flares (X-rays up to 10^{-4} W/m^2); October 24-25, period of high (Kp ~ 6) geomagnetic activity with high lightning activity; October 28-29, complicated period when two solar flares occurred simultaneously with high geomagnetic activity (Kp ~9); October 29-30, one but powerful enough (~ 10^{-3} W/m^2) solar flare with a long period of high geomagnetic activity and GCR Forbush decrease; October 30-31, a period of high geomagnetic activity with short-time lightning activity [Mikhailova et al., 2014].

Fig. 4 and 5 allow us to trace power spectra variations of the parameters under consideration from 21 to 31 October (vertical cross sections) and the relation of these parameters during separate time intervals (horizontal cross sections).

We consider the variations of weather parameter power spectra, those of air temperature and humidity (ST and SV).

In fair weather conditions on October 21-22, before a strong solar flare, thermal radiation with the known diurnal variations penetrate to the Earth via the so called spectral window (infra-red and visible radiation and far-UV radiation) and determine the air temperature and humidity power spectra. In the result, thermal tidal wave components, S_{max} in T ~ 24 h and weak additional maxima in T ~ 12 and 48 h, present in their spectra (ST and SV).

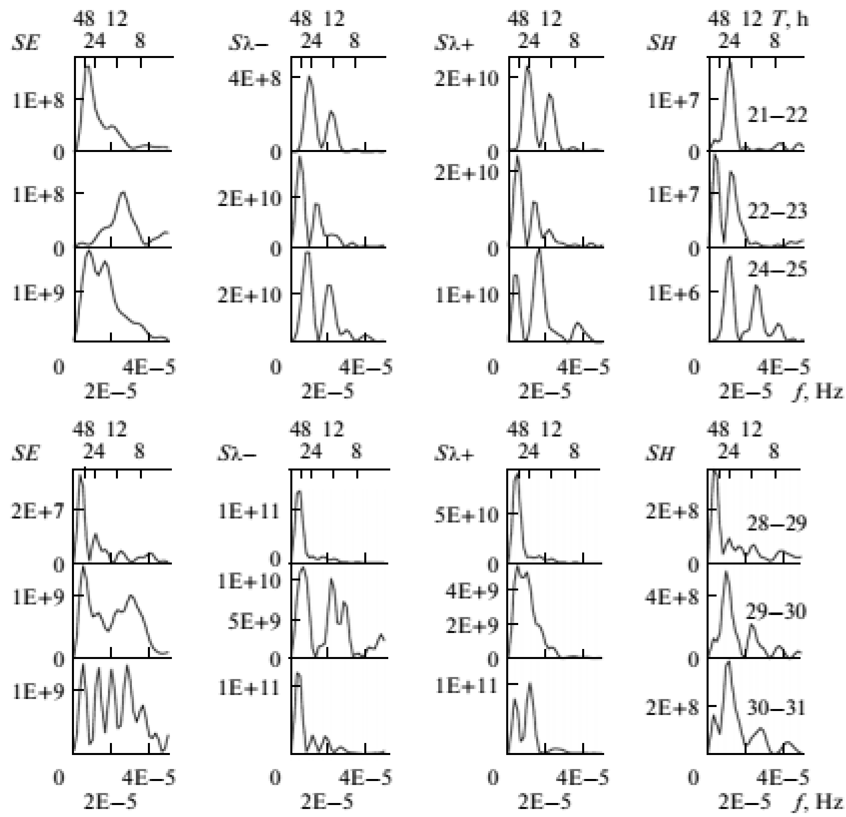

Fig. 4 Sequence of spectral power density of the parameters shown in Fig. 3. Frequency f, Hz, is shown at the bottom axis and the corresponding periods T are at the upper axis.

With the increase of solar activity on October 22-23, a frequency-unclear component with T~ 48 h appears in the temperature spectrum ST, which becomes a prevailing one during the magnetic storm on October 24-25. The intensity of the components with T ~ 12 and 24 decreases significantly. As the solar and the geomagnetic activities develop, the both components with T ~ 24 and 48 h take turns to increase and to decrease but are constantly presented in ST spectrum. Air humidity power spectra (SV) also undergo complicated changes. Their character additionally varies due to the precipitation during lightning processes on October 24, 30 and 31. Completely a different character is observed in air pressure variations (SP) within the whole period of development of solar and geomagnetic processes, a prevailing component with T ~ 48 with a weakly determined component on T ~ 24 h is presented. In this case, the intensity of this maximum changes insignificantly except for the period on October 29-30 when spectral density increases by almost an order of magnitude.

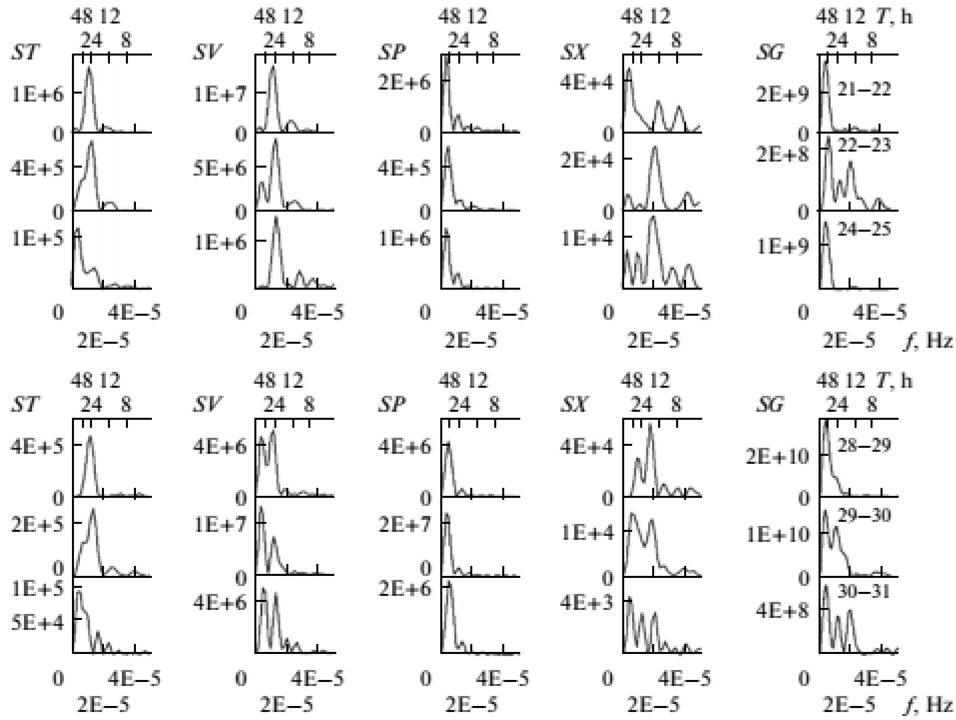

Fig. 5. Curve sequence for spectral power density of the parameters illustrated in Fig. 3. Frequency f, Hz, is at the bottom abscissa axis, and the corresponding periods T are at the upper axis.

Now we consider the X-radiation power spectra of the Sun and that of the galactic cosmic rays (SG).

It is known [Fontenla et al., 2004; Woods et al., 2004] that the presence of an active area on the Sun disk increases the radiation flux in the whole range of electromagnetic emission. To estimate the wave processes on the Sun, we apply the X-radiation intensity records that characterizes flare intensity. (In our case, it is quite a rough approach to the estimate of near-ground atmosphere processes). Analysis of SX spectra shows the following: in fair weather conditions on October 21-22 there is a wide set of the components and thermal tidal waves (24, 12, 8 h), and planetary scale waves (T ~ 48 h) in SX spectrum. As solar and geomagnetic activity develops, the spectral content remains but the intensity of different components changes significantly. We can suppose that such a character of the spectrum also remains in the band of atmospheric transparency window through which additional heat inflow penetrates to the ground. It affects air temperature and humidity.

During this period, a complicated character is also observed in the power spectra of galactic cosmic rays (SG). In fair weather conditions on October 21-22, a relatively weak decrease in GCR flux is observed in GCR time variation (Fig. 3, curve 10). It is caused by a preceding solar flare on October 20. The following event of GCR flux decrease accompanied the flare on October 23 that was also reflected in the spectrum by the increase of the component with T ~ 48 h. During the significant decrease of the flux on October 29, this component intensity increased by an order in magnitude compared to the period of October 21-22. During the recovery stage, the components with T ~ 12, 24 h were added to the prevailing component with T ~ 48 h in SG power spectra. Since the GCR flux intensity decrease is associated with the intensification of the solar wind blocking these fluxes, we can suppose that GCR spectral content is determined by the process periodicity on the Sun which also manifests in X-ray spectral content.

We consider the power spectra of atmospheric electricity parameters, such as, air electrical conductivity $S\lambda_-$ and $S\lambda_+$ and electric field strength SE. In fair weather conditions on October 21 – 22, a wide intensity maximum in the period band of 24 h <T< 48 h and a weaker maximum with T ~ 12 prevail in SE power spectrum. During the solar activity on October 22 and 23, the spectrum change in such a way that almost the whole power was concentrated in the period band of 12-24 h. Moreover, during the solar flares on October 28-29, the power spectrum was enlarged by a component in a wide period range of 12-48 h. During the magnetic storms on October 24-25 and 29-30, the components with T ~ 48 h prevail in the spectrum. Their intensity exceeds the corresponding component on October 21-22 by one order in magnitude. The complicated character of SE spectrum on October 24-25 and 30-31 is associated with lightning activity effect that was observed at that time.

A similar complicated character of $S\lambda_-$ and $S\lambda_+$ power spectra was observed on those days. In fair weather conditions on October 21-22, two components of 12 and 24 h were detected in the spectrum. They coincided with the periods of thermal tidal waves. However, as the solar activity increased on October 22-23, the increase of the prevailing component with T ~ 48 h was observed at the background of the components with T ~ 24, 12, 8 h.

DISCUSSION

In the framework of ball condenser model, current density in the atmosphere is determined by the expression:

$$J=\lambda E+\rho V+D_t \nabla \rho+\Sigma J_s$$

where $\lambda = e\Sigma\left(n_{i+}u_{i+}+n_{i-}u_{i-}\right)$, $n_{i\pm}$ is the concentration of positive and negative ions prevailing in the lower atmosphere; $u_{i\pm}$ is the ion mobility: λE is the conductivity current determined by lightning generator; ρ is the bulk charge; V is the medium motion velocity; D_t is the diffusion turbulence coefficient. The latest term of the expression includes points of different sources, in particular, precipitation currents $J = \Sigma q_m n_m v_m$, where q_m is the charge, n_m is the concentration, v_m is the particle fall velocity during precipitation, respectively; as well as global source currents (SCR and GCR) contributing into the global electric circuit.

In fair weather conditions, solar activity effect on the current density J and, in particular, on electric field strength manifests in several ways. Firstly, through the air conductivity change that is determined by ion concentration and their mobility. Due to the low temperature in October (curve 5, Fig. 3), at the presence of snow cover and precipitation (curve 7, Fig. 3), the outflow of underground air containing radon is delayed [Moses et al., 1960]. The contribution of the galactic cosmic rays into the lower troposphere is insignificant, thus, when ion concentration changes weakly, the air conductivity is determined by ion mobility which depends on air temperature [Bricard, 1965]. Moreover, the relation with the solar activity manifests in the effects of sunrise and sunset through the influence of the local convective generator [Smirnov et al., 2012; Smirnov, 2013] when with temperature increase, convective and turbulent thermal currents contributing to the current density (terms ρV and $D_t\nabla\rho$) gain in strength. This relation with the solar activity manifested in concurrent variations of the power spectra of temperature (ST), humidity (SV), electrical conductivity ($S\lambda_{\pm}$), and partially in SE where the components of thermal tidal waves are presented. Additionally, the solar activity effect manifested through the influence of cloudiness and precipitation which were observed at Paratunka observatory during the period under consideration more episodically than periodically. Their contribution manifested in the electrical conductivity variations (curves 2 and 3, Fig. 3).

In disturbed conditions during powerful solar flares, the global atmospheric ionizers come into action in the GEC, they are: solar (SCR) and galactic (GCR). After a powerful solar flare on October 26, the SCR main streams in the Northern Hemisphere increased from 1 to ~ 10^2 on October 27, and to ~ 10^3 h/sm^2 s sr on October 28-29 during relatively calm GCR variations (curve 9, Fig. 3). Moreover, as it is known that the hard cutoff boundary for SCR descends. That could not but cause the growth of ion concentration in the troposphere and, consequently, the conductivity in GEC. Evidently, this process can qualitatively explain the high constant level of electrical conductivity during a day on October 27 and 28 and the presence of the prevailing component with T ~ 48 h in $S\lambda_{\pm}$ and SE spectra. The GCR Forbush decrease at 16:00 UT (curve 10, Fig. 3) suppressed the effect of SCR and expanded the $S\lambda_{\pm}$ and SE power spectra into the period region (T ~ 48 h). In the result, during this anomalous period of the solar activity, global sources of atmosphere ionization suppressed the effects of local sources, those of the convective generator, clouds and precipitation.

CONCLUSIONS

The investigations of the power spectra of the near-ground atmpspheric electric characteristics at the mid-latitudinal observatory during solar events showed the following:

- large oscillations of electric field were observed. They coincided with the sudden commencement of the magnetic storm. Such disturbances are likely to be caused by induction processes;
- decrease of air electric conductivity is possibly caused by Forbush effect. Galactic cosmic ray flux which ionizes the atmosphere decreased;
- during strong solar flares and a magnetic storm, the maxima are shifted in the direction of larger periods in the electric field power spectra. The component with T ~ 48 h increased by an order in magnitude in comparison to fair weather conditions;
- in the power spectra of galactic cosmic rays accompanying strong solar flares, the component with T ~ 48 h prevailed. It was intensified by an order in magnitude during Forbush decrease. Simultaneous increase of the components with T ~ 48 h in the power spectra of air electrical conductivity and electric field strength indicates the fact that during strong solar flares and magnetic storms, the galactic cosmic rays are mainly the active ionizers of the lower troposphere.

REFERENCES

Bricard, J., 1965: Action of radioactivity and pollution upon parameters of atmospheric electricity. *Problems of Atmospheric and Space Electricity*. Elsevier, Amsterdam, 82–117.

Fontenla, J.M., J. Harder, G. Rottman, T.N. Woods, G.M. Lawrence, and S. Davis, 2004: The Signature of Solar Activity in the Infrared Spectral Irradiance. *The Astrophysical Journal,* **605**, L85-L88.

Imyanitov, I.M., 1957: *Instrumentation and methods to investigate atmospheric electricity*. Gostechizdat, Moscow, 483 pp.

Mikhailova, G.A., O.V. Kapustina, and S.E. Smirnov, 2014: Effects of solar and geomagnetic activities in variations of power spectra of electrical and meteorological parameters in the near-Earth atmosphere in Kamchatka during October 2003 solar events. *Geomagnetism and Aeronomy*, **54(5)**, 645-654. https://doi.org/10.1134/S0016793214050119

Moses, H., A.F. Stehnly, and H.F Lucas, 1960: The effect of meteorological variables upon the vertical and temporal distributions of atmospheric radon. *J. Geophys.Res.,* **65(4)**, 1223-1238.

Roble, R.G., 1985: On solar-terrestrial relationships in atmospheric electricity. *J. Geophys.Res.,* **90(D4)**, 6000–6012. https://doi.org/ 10.1029/jd090id04p06000.

Rycroft, M.J., K.A. Nicoll, K.L. Alpin, and R.G. Harrison, 2012: Recent advances in global electric circuit coupling between the space environment and the troposphere. *J.Atmos.Sol.Terr.Phys.,* **90-91**, 198–211. https://doi.org/10.1016/j.jastp.2012.03.015.

Siingh, D., R.P. Singh, V. Gopalakrishnan, C. Selvaraj, and C.P. Panneerselvam, 2013: Fair-weather atmospheric electricity study at Maitri (Antarctica). *Earth Planets Space,* **65(12)**, 1541–1553, doi:10.5047/eps.2013.09.011

Smirnov, S.E., G.A. Mikhailova, and O.V. Kapustina, 2012: Problem of the nature of the sunrise effect in diurnal variations in the electric field in Kamchatka: 1. Time variations in the electric field. *Geomagnetism and Aeronomy.* **52(4)**, 507-512. https://doi.org/10.1134/S0016793212040135.

Smirnov, S.E., 2013: Influence of a convective generator on the diurnal behavior of the electric field strength in the near-Earth atmosphere in Kamchatka. *Geomagnetism and Aeronomy,* **53(4)**, 515-521. https://doi.org/10.1134/S0016793213040142.

Smirnov, S.E., G.A. Mikhailova, and O.V. Kapustina, 2014: Variations in electric and meteorological parameters in the near-Earth's atmosphere at Kamchatka during the solar events in October 2003. *Geomagnetism and Aeronomy,* **54(2)**, 240-247. https://doi.org/10.1134/S0016793214020182.

Smirnov, S., 2014: Reaction of electric and meteorological states of the near-ground atmosphere during a geomagnetic storm on 5 April 2010. *Earth, Planets and Space,* **66**, 154. https://doi.org/10.1186/s40623-014-0154-2

Woods, T.N., F.G. Eparvier, J. Fontenla, J. Harder, G. Kopp, W.E. McClintock, G. Rottman, B. Smiley, and M. Snow, 2004: Solar irradiance variability during the October 2003 solar storm period. *Geophysical Research Letters,* **31**, L10802. https://doi.org/10.1029/2004gl019571.